Behaviour of cold-formed dimpled columns under lateral impact

Ce Liang [a,*]Chang Jiang Wang [a], Martin English [b], Diane Mynors[a]

[a] Department of Engineering and Design, School of Engineering and Informatics, University of Sussex, Brighton, BN1 9QT, United Kingdom

[b] Hadley Group Technology, Hadley Industries plc, Downing Street, Smethwick, West Midlands, B66 2PA, United Kingdom

[*] Corresponding author at: Richmond Building, Department of Engineering and Design, School of Engineering and Informatics, University of Sussex, Brighton, BN1 9QT, United Kingdom. *Email address: cl305@sussex.ac.uk*

Abstract

The UltraSTEEL® forming process forms plain steel sheets into dimpled steel sheets. During the forming process both geometry and mechanical properties are considerably altered. This study aims to understand the response of the dimpled steel columns to low velocity lateral impact loads. Explicit finite element (FE) models were created and validated, including boundary conditions, element types and element sizes. Plain, dimpled columns and columns with dimpled geometry and plain material (DGPM) were analysed under lateral impact, to find out the difference between plain and dimpled columns, and the influence of the introduced dimpled geometry. Comparisons were made based mainly on the mean impact force, crush efficiency, and ability to maintain stability. A series of numerical analysis was carried out under different axial compressive loads. The dimpled columns have shown an up to 32.5% greater mean force and an up to 24.4% greater crush efficiency over the plain ones. The dimpled columns have also shown a better stability under axial compressive loads. A further investigation on the support conditions indicated that the dimpled geometry contributes to the reduction of the maximum impact force and therefore increasing the crush efficiency, where at least one end of the column is fully fixed.

Keywords

Explicit dynamics FE analysis; UltraSTEEL dimpled material; Square hollow section (SHS); Lateral impact; Energy absorption

1. Introduction

Hollow tubular members are widely used in many infrastructures. It has been identified in some previous researches that hollow tubular members are prone to transverse impact loading [1]. Past research and statistic data have revealed that accidental collision is one of the main causes of structural failure [2, 3]. During the collision, the structural components are exposed to the operating axial compressive load as well as the lateral impact loads [4]. The collision energy is absorbed by the tubular members subjected to bending conditions. Kecman [5] has studied the bending collapse behaviour of rectangular section columns when subjected to quasi-static lateral loads. Kecman's [5] study has established the foundation for the analytical prediction of the response of rectangular section columns to lateral quasi-static loads, and can be further extended to analytically predict the columns' behaviour under lateral impact load. Liu and Jones [6] experimentally studied the behaviour of steel and aluminium clamped beams under transverse impacts. Their study was further extended by Yu and Jones [7], who have taken the materials' strain rate sensitivity into account. Wierzbicki et al. [8] extended the super folding element (SFE) method to theoretically predict columns' behaviour in the case of bending and combined bending/compression loading [8]. In all these previous proposed analytical methods [5-8], the columns were assumed to be plain and have constant thickness, and no theoretical prediction method for concave-convex surface columns have been developed. Zeinoddini et al. [9, 10] introduced an axial compressive load under lateral impacts through an experimental study. This experimental study was then repeated by running FE simulations. Their experimental and numerical results were adopted to validate the FE models in the present study. Based on the research of Zeinoddini et al. [9, 10], Al-Thairy and Wang [4] carried out a study by developing FE models to simulate the

transverse impact behaviour and failure modes of axially compressed tubes subjected to transverse impact. Those studies [4, 9, 10] have all pointed out the significant influence of axial compressive loads on the failure modes, and similar boundary and loading conditions were investigated in the present study.

In recent years, there is a particular interest in improving the resistance of tubular members to lateral impact loads. Some research focused on strengthening tubular members with various types of fillers [11-16], such as concrete, foam or metal honeycomb core. By contrast, some research focused on tubular members strengthened by applying carbon fibre reinforcement [17-19]. It has been reported that the mean impact forces and/or crush efficiencies can be effectively increased by using those design strategies [11-19]. Although different strategies have been studied to improve the energy absorption performance of structural members subjected to lateral impact loads [11-19], all those studies were limited to columns with plain surfaces, and the effects of introducing concave-convex geometry on the surfaces have not been previously investigated.

Dimpled steel columns are formed from plain mild steel sheets by the UltraSTEEL® cold-roll forming process developed by Hadley Industries plc [20]. In this forming process, plain mild steel coil is progressively fed into a pair of rollers with rows of specifically shaped teeth and formed into dimpled steel sheets, as shown in Fig. 1. [21]. Dimpled sheets are then formed into desired profiles by passing through a series of rolls or press braking. Several previous numerical and experimental research has revealed that the strengths of dimpled steel sheets are significantly greater than those of the original plain steel sheets [21-27]. The increase in strength is mainly due to work hardening developed throughout the forming process. The increase in strength was accurately predicted by Nguyen et al [22] through FE simulations. Previous research

mainly focused on the UltraSEEL® forming process and dimpled structures' behaviour under quasi-static loads. Liang et al. [23] extended previous research and investigated the dimpled structures' response to dynamic axial impact loads numerically and experimentally. The FE models were developed and validated to predict dimpled structures' behaviour under impact loading conditions. An optimization study on the UltraSTEEL® forming process was also carried out for achieving higher crashworthiness [23]. However, the behaviour and energy absorption performance of dimpled tubular members subjected to lateral impact loads have not been studied.

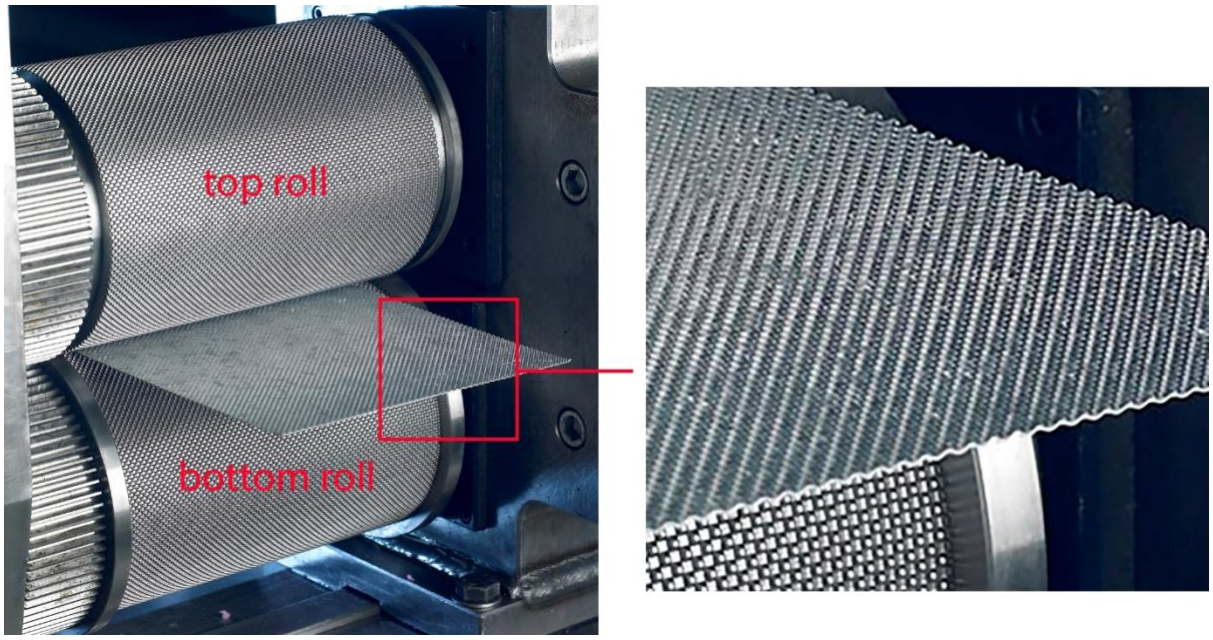

Fig. 1. The UltraSTEEL® forming rollers and dimpled steel sheet.

This paper aims to investigate the behaviour of thin-walled dimpled steel columns under lateral impact loads. To achieve this aim, numerical simulations based on the validated FE models were conducted. In this study, the dimpled column was analysed under various loading and support conditions. Comparisons between dimpled and plain steel columns subjected to lateral impacts were conducted.

2. Finite element modelling

In this study, the explicit dynamics finite element code integrated in Ansys Workbench 17.1 [28] was employed to simulate the plain and dimpled steel columns' response to lateral impact loads. This explicit dynamics FE code is commonly used to deal with non-linear simulations involving complex contact interactions. The specific employment of this code to simulate the behaviour of dimpled steel structures with medium strain rate (between 0.1 and 100 s^{-1}) was validated by Liang et al. [23]. Main challenges about numerical analysis for dimpled structures under dynamic loads are constructing the geometrical model, selecting element types and sizes, and assigning appropriate material properties. In [23], the FE method was developed to resolve these issues. Experimental tests were conducted to validate the FE method. Good agreement was found in terms of failure mechanisms and impact forces. Therefore, only additional features of the numerical models will be introduced in this paper.

2.1 Material properties

The materials' mechanical properties were obtained from quasi-static tests, following the appropriate British Standard [29]. The quasi-static tensile testing procedures are presented by Nguyen et al. [24]. The plain and dimpled samples used in the tensile test were originated from the same coil of steel. The tensile test results are shown in Fig. 2, where the engineering yield and ultimate strengths of the dimpled steel are around 17% and 9% higher than the plain steel, respectively. True stress and strain were input into the programme.

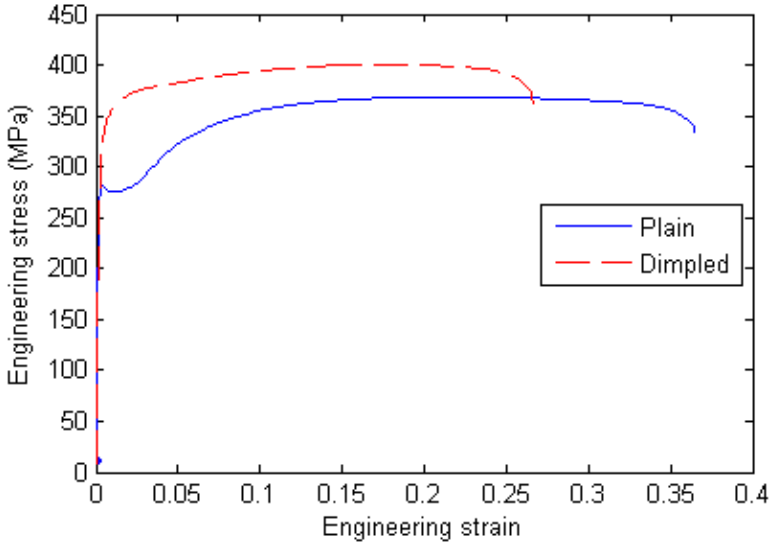

Fig. 2. Quasi-static engineering stress-strain curves for plain and dimpled materials

It has been pointed out in a number of research papers that materials' strain rate effect plays an important role in energy absorption when structural components are subjected to dynamic loads. In this study, the Cowper-Symonds material model was adopted to characterise the strain rate sensitivity of plain and dimpled steel, as shown in equation 1. The yield strengths σ_y are 278 MPa and 348 MPa for plain and dimpled materials, respectively. For both plain and dimpled materials, the coefficients B, n, D and q are 383 MPa, 0.6036, 40.4 and 5, respectively.

$$\sigma^d = \left(\sigma_y + B\varepsilon^n\right)\left[1 + \left(\frac{\dot{\varepsilon}}{D}\right)^{1/q}\right] \quad (1)$$

2.2 Samples and boundary conditions

The square hollow section (SHS) columns adopted in this study are 500 mm long and 33 mm wide. The thickness is 1 mm for plain column walls and 0.959 mm for dimpled column walls, due to the stretched surface after the forming process. To obtain the geometric model of the dimpled plates, the UltraSTEEL® forming process was firstly

simulated using Ansys Mechanical APDL, based on a small square plate with symmetric boundary conditions applied, as described in [24]. The resultant nodal coordinates were exported to construct the generic geometric model of dimpled plates. The geometric models of the dimpled columns were then created by patterning the generic dimpled models. As shown in Fig. 3, the columns were fully fixed at one end and roller supported at the other end. To represent this support condition, all DOFs of the fully fixed end were constrained, while translational DOFs of the roller supported end were constrained along x and y directions. The external loads were applied in two stages. In the first stage, a quasi-static constant axial compressive load was applied on the roller supported end. When selecting the axial compressive loads, it was ensured that the column did neither buckle nor yield solely under the axial compressive load. In the second stage, a 4.9 kg impact mass with an initial velocity of 8 m/s along y-axis was applied, providing an impact energy of 156.8 J. The indenter was considered as a rigid body and translational DOFs of the impact mass were constrained along x and z directions, in order to represent the impact mass sliding along a straight trajectory. As shown in Fig. 3, the end of the indenter is semicircle and the radius is 10 mm, and the initial contact location was at the mid-span of the column. In the FE simulations, the automatic node-to-surface contact function was used to compute the contact between the indenter and the column, and the trajectory detection method was used. Symmetric boundary conditions were applied to the FE model along the axial direction.

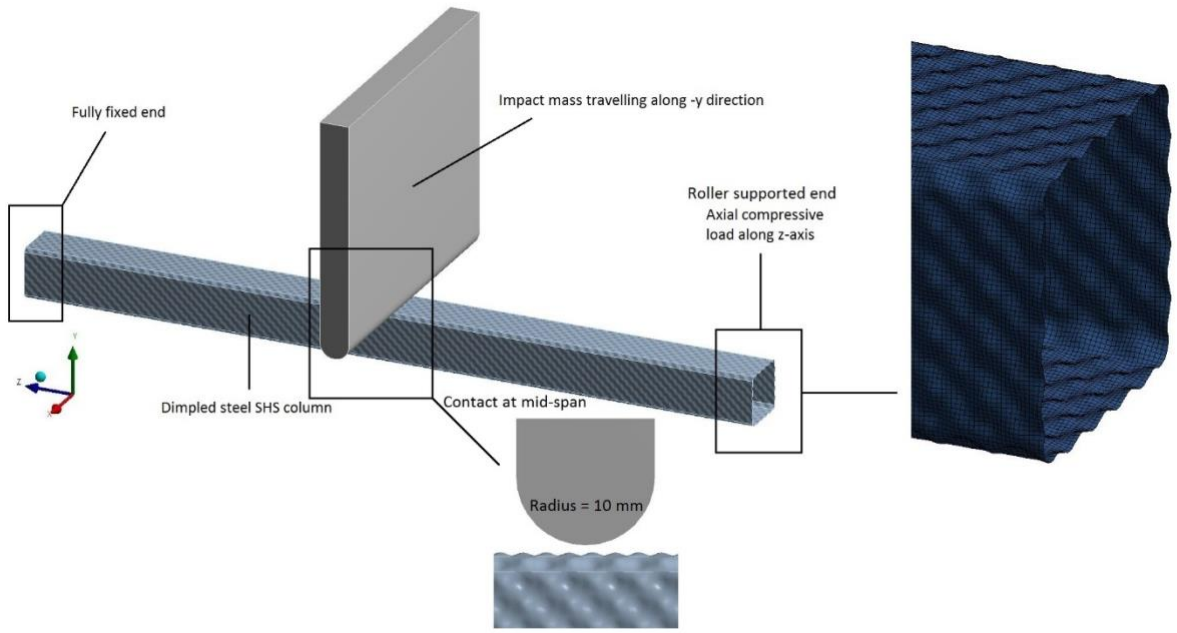

Fig. 3. FE model of the dimpled column and impact mass

2.3 Elements and mesh

The impact mass was constructed using 8-node solid elements. The columns were modelled using full-integration 4-node shell elements with five integration points throughout the thickness. Uniform thickness and homogeneous material properties were assigned to the entire column, while in reality the thickness and mechanical properties slightly vary within the material. In this section, tensile tests were simulated based on solid element and shell element dimpled FE models, and a comparison was made. Fig. 4(a) and 4(b) show the solid and shell elements numerical results, respectively. Fig. 4(c) shows experimental and numerical engineering stress-strain curves of the dimpled steel material. It reveals that the difference due to the approximation in thickness and mechanical properties can be neglected.

A mesh density convergence study was performed to determine the appropriate element sizes for providing sufficiently accurate results as well as to minimize the

requirement for computational resource. It is found that results were converged when the element size was 1 mm, however geometrical distortion was identified due to the continuous wavy geometry. As a result, the element sizes adopted were 1 mm and 0.55 mm for plain and dimpled models, respectively.

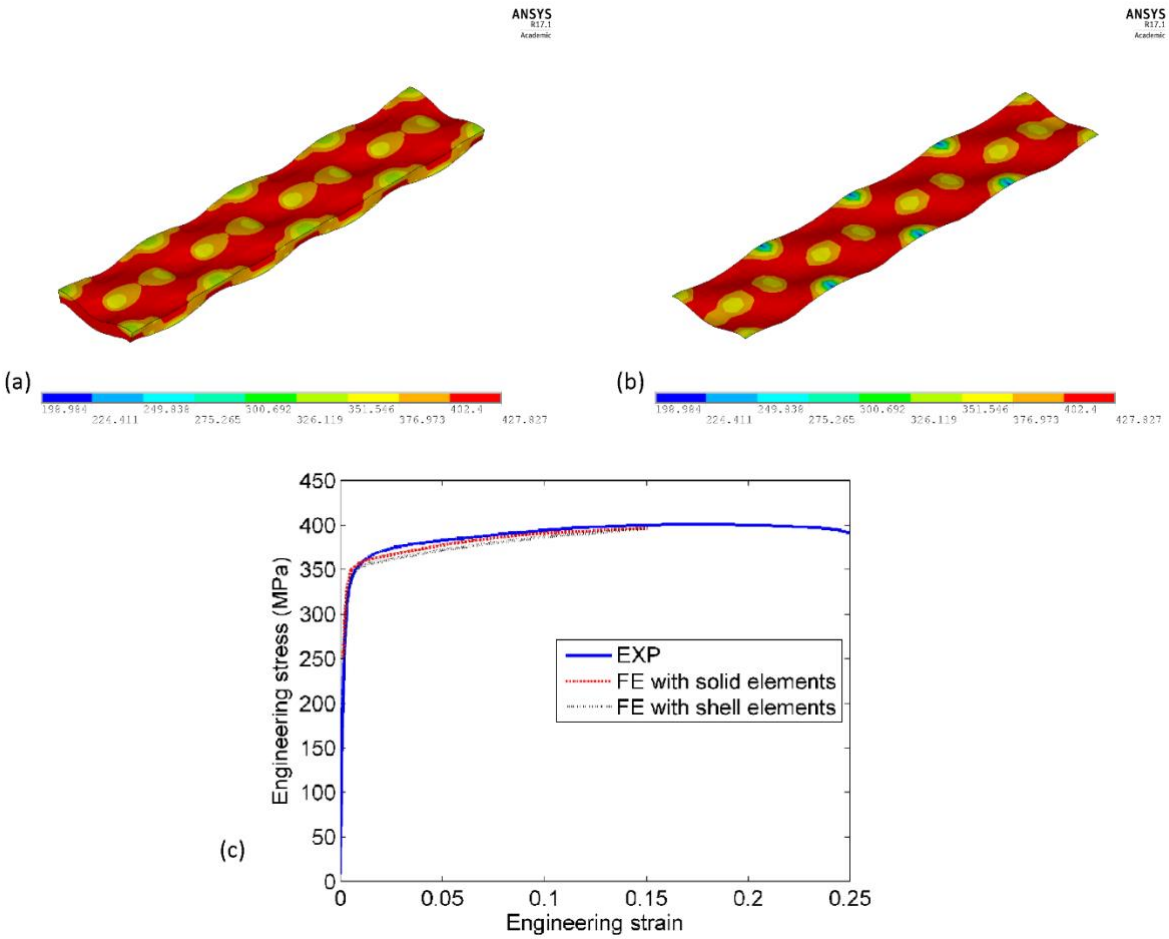

Fig. 4. Simulated tensile test with (a) 8-node solid elements, (b) 4-node shell elements, (c) experimental and numerical tensile test results for the dimpled steel

2.4 Validations

Although using the FE method to simulate the dimpled columns' response to low-velocity impact loads has been previously validated [23], further validations are required to ensure that the boundary conditions are correctly applied. The

experimental tests and numerical simulations conducted by Zeinoddini et al. [9, 10] were replicated using the FE method introduced above, for their similar support and loading conditions. In those tests, a pre-compressed steel tube was hit by a 25.45 kg impactor with an impact velocity of 7 m/s at the mid-span. The FE model used in the present study to simulate the tests in [9] is shown in Fig. 5, where the axial compressive loads were set to be 0 and 50% of the squash load. The numerical impact force and deformed shapes in the present study are compared against those reported by Zeinoddini [9, 10] in Figs. 6 and 7. It was observed that the current numerical results agreed well with the experimental and numerical results in [9, 10]. The difference in the force-time curves did not have a significant effect on the mean force, maximum force or crush efficiency. Therefore, the FE method used in the present study can be considered to output reasonably accurate results.

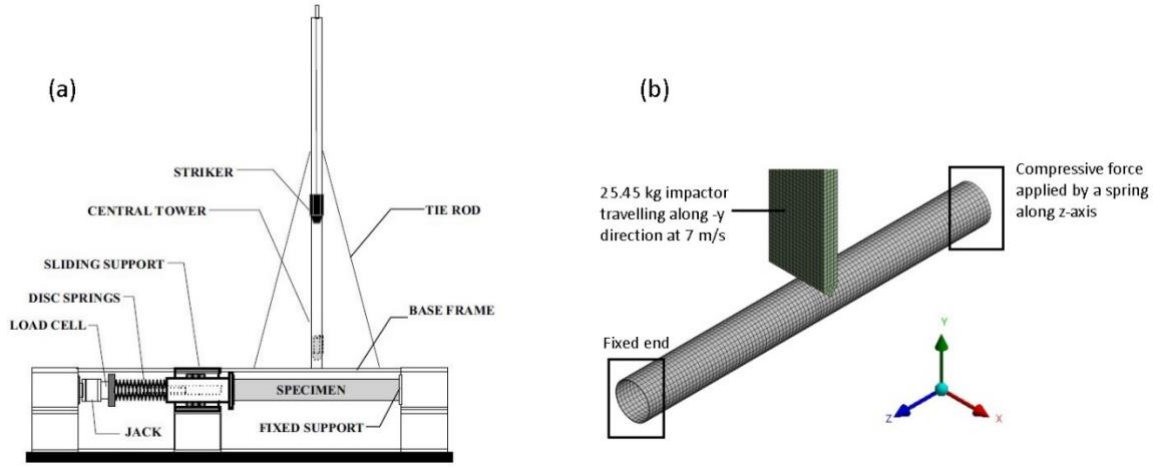

Fig. 5. (a) Schematic plot of the experimental setup [9] and (b) FE model used in the present study

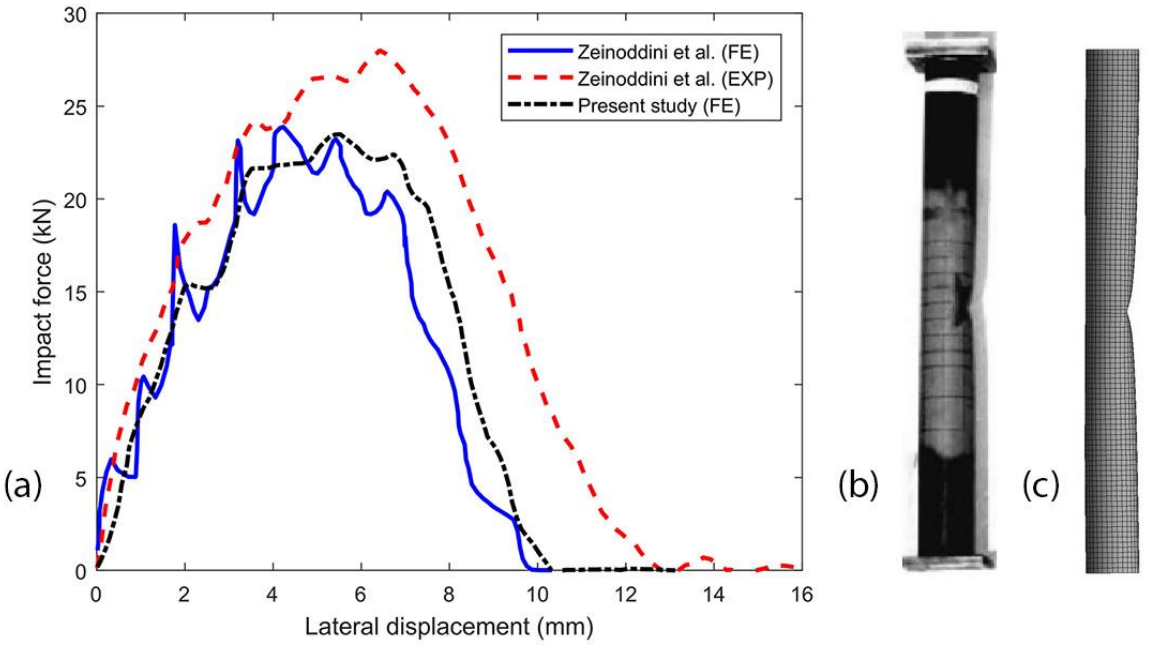

Fig. 6. (a) Historical impact forces, (b) experimental deformed shape in [9] and (c) numerical deformed shape in the present study when axial force = 0

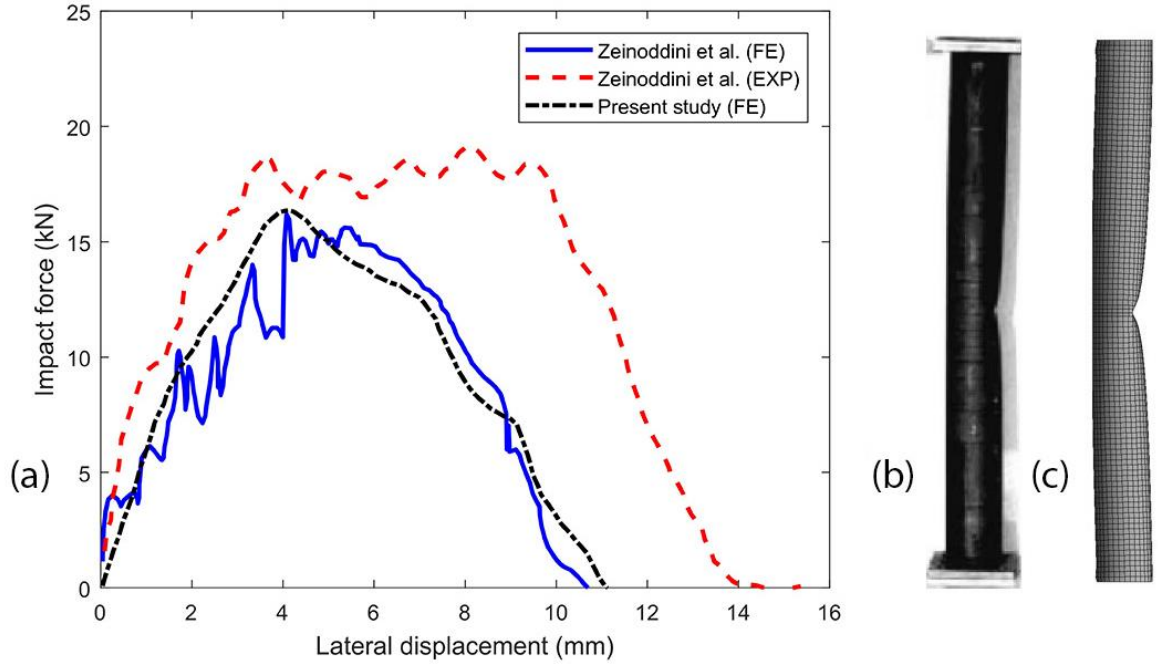

Fig. 7. (a) Historical impact forces, (b) experimental deformed shape in [9] and (c) numerical deformed shape in the present study when axial force = 50% squash load

3. Results and discussion

As introduced in section 2.1, the initial impact velocity was set to be 8 m/s and impact mass was set to be 4.9 kg in this study. Besides the results for plain and dimpled columns, the results for columns with dimpled geometry and plain material properties (DGPM) were computed and analysed. The DGPM columns were not physically formed. The purpose of adding the imaginary DGPM samples is to eliminate the effects of the material properties, and therefore highlight the effects of the dimpled geometry.

3.1 The failure mechanisms

Fig. 8. shows the force-deflection curves of the plain, dimpled and DGPM columns when the axial compressive load is 6 kN, where the horizontal axis refers to the local lateral displacement at the impact location. Similar patterns are obtained when a greater or smaller axial compressive load is applied. As shown in Fig. 8, for plain columns, three peak forces can be observed before the residual force phase. However, for dimpled and DGPM columns, the 1st peak force is not very distinct and therefore may be neglected. The deformed shapes and equivalent plastic strains for the dimpled column at the 1st peak force, 2nd peak force, the maximum peak force and residual force phases are shown in Fig. 9. Models presented in Fig. 9. were simplified using symmetrical boundary conditions. The 1st peak force appears when the contact between impactor and column starts. The 2nd peak force appears while local buckling around the impact location is being developed. The maximum peak force appears when the buckling around the fixed end initiates. The global failure modes for plain, dimpled and DGPM columns are similar. Additionally, the equivalent plastic strain distributions for dimpled and DGPM columns are similar to each other,

but considerably different from the plain column. The yielding effect is more concentrated in dimpled and DGPM columns. As shown in Fig. 10, when the 1st peak force appears, the surface area of yielded region in the plain column is about 160 mm^2, comparing with 51.4 mm^2 in the equivalent dimpled and DGPM columns. When the maximum peak force appears, comparing with the continuous and smooth strain distribution near the fixed end for the plain column, as shown in Fig. 11, the strain is distributed along the diagonal direction of dimples for dimpled and DGPM columns, as shown in Fig. 9(c).

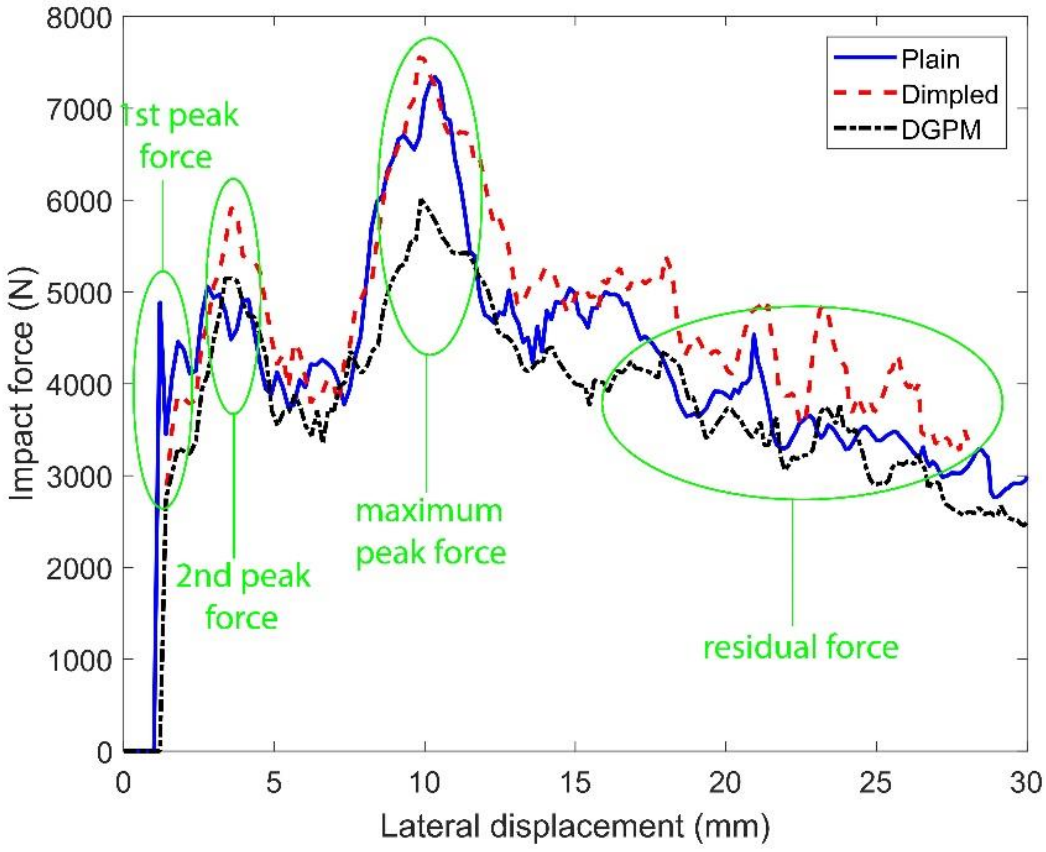

Fig. 8. Typical impact force – lateral displacement patterns

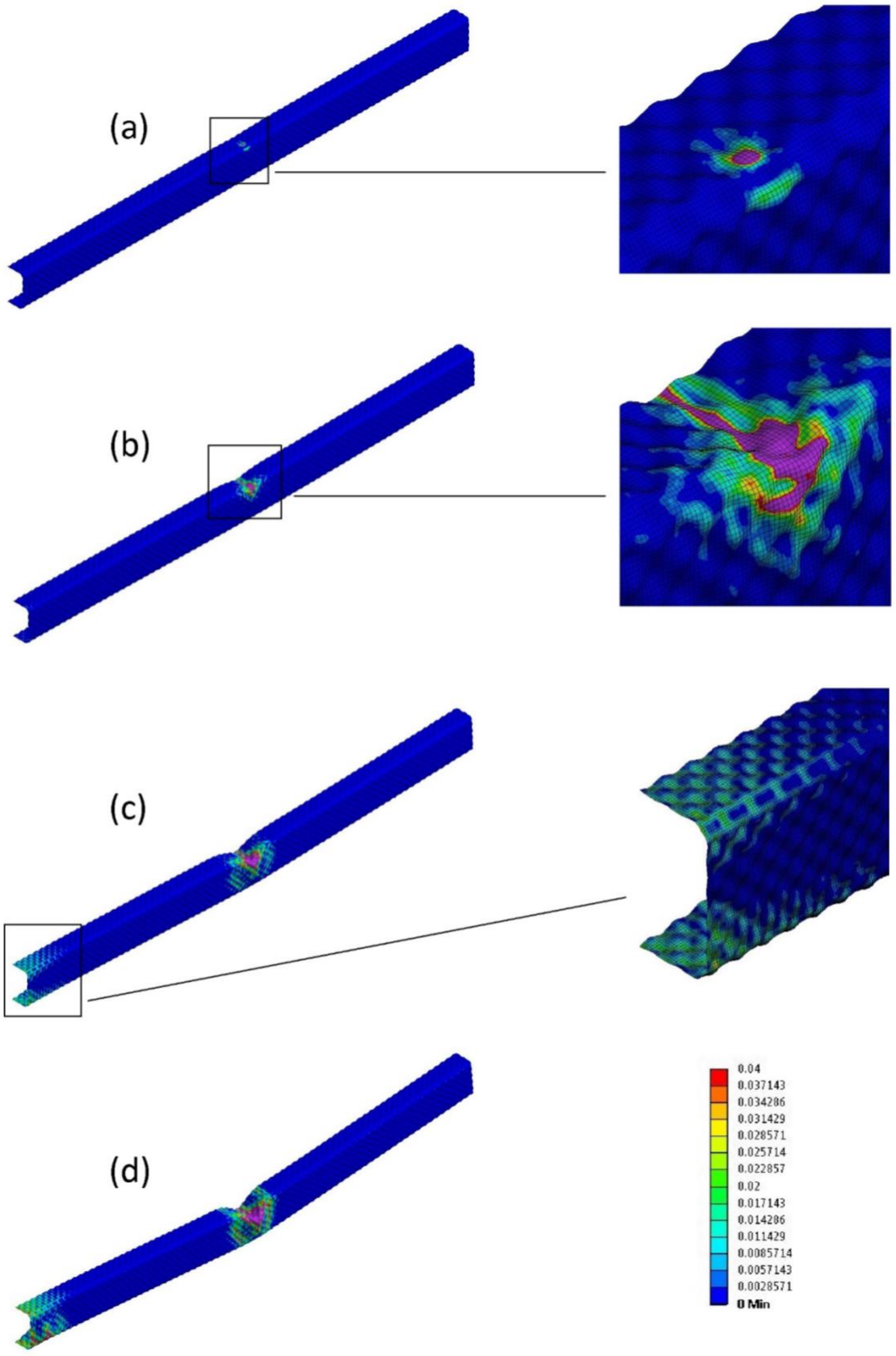

Fig. 9. Deformed shapes and plastic strains of the dimpled column at (a) 1st peak force, (b) 2nd peak force, (c) maximum peak force and (d) residual force phases

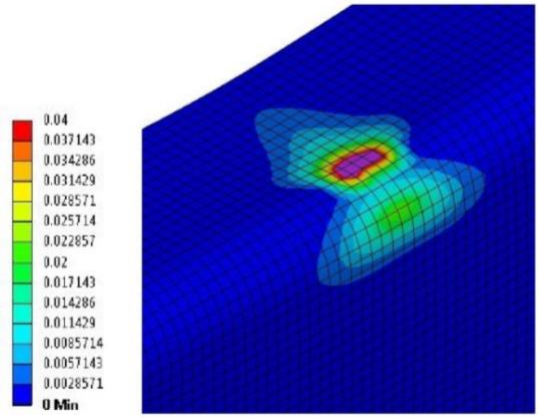

Fig. 10. Plastic strain near the impact location of the plain column at the 1st peak force

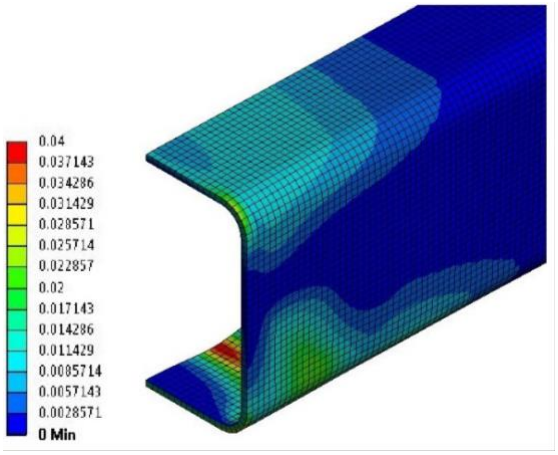

Fig. 11. Plastic strain near the fixed end of the plain column at the maximum peak force

3.2 Parametric study: effects of axial compressive load

In most engineering applications, lower maximum impact forces are usually preferred to reduce the damage to passengers or infrastructures, while greater mean impact forces are usually preferred for high energy absorption capacity. Therefore, the variable crush efficiency η_c, as defined in equation 2, was employed to evaluate the energy absorption performance of the columns in this study.

$$\eta_c = {}^{P_{mean}}/_{P_{max}} \quad (2)$$

In the FE simulations, axial compressive loads up to 31% of the squash loads were applied. The variations of mean force, peak force, 2nd peak force and crush efficiency against the axial compressive load are shown in Fig. 12 and Table 1. As shown in Fig. 12(a), the mean impact forces drop as the axial compressive load increasing. Dimpled columns have greater resistance than plain and DGPM columns. The dimpled geometry does not significantly influence the mean impact force, especially under greater compressive loads. The dimpled columns' mean force is 10.9%-32.5% and 16.6%-34.2% greater than equivalent plain and DGPM columns' respectively, as the compressive load varying. The higher mean impact force of dimpled columns imply that it is feasible to replace plain columns with thinner dimpled columns, without sacrificing the energy absorption capacity, which is beneficial for weight reduction. However, the potential weight reduction will not be quantified in the present study. Fig. 12(b) reveals that the dimpled columns' peak impact forces are slightly greater than plain columns' and significantly greater than DGPM columns'. The comparison between plain and DGPM samples reveals that the dimpled geometry reduces the maximum impact force by up to 20.7%. The reason is that the peak force appears when buckling initiates near the fixed end, and the dimpled geometry has caused under-developed yielding effect near the fixed end, as described in section 3.1. Fig. 12(c) suggests that the 2nd peak forces are not significantly influenced by axial compressive loads. Additionally, the dimpled geometry does not appear to affect the 2nd peak force, either. Fig. 12(d) shows the variation of crush efficiency against compressive loads, which is a combined result of the mean impact force and peak impact force. It is found that dimpled geometry has caused an increase between 12.6% and 20.4% in crush efficiency, mainly due to the reduced peak impact force.

When suffering combined axial compressive and lateral impact loads, there is a potential risk that the axial compressive load will squash the column after the impact energy being fully absorbed, and the column will therefore lose its stability. The critical compressive load P_c, is defined as the maximum compressive load under which the column can still maintain stability after absorbing a specific amount of impact energy. The critical compressive loads for plain, dimpled and DGPM columns were determined on a trial and error basis. As shown in table 1, although the dimpled columns did not show an advantage in terms of the ratio P_c/P_y, the critical compressive load is about 11.1% greater than its plain counterpart.

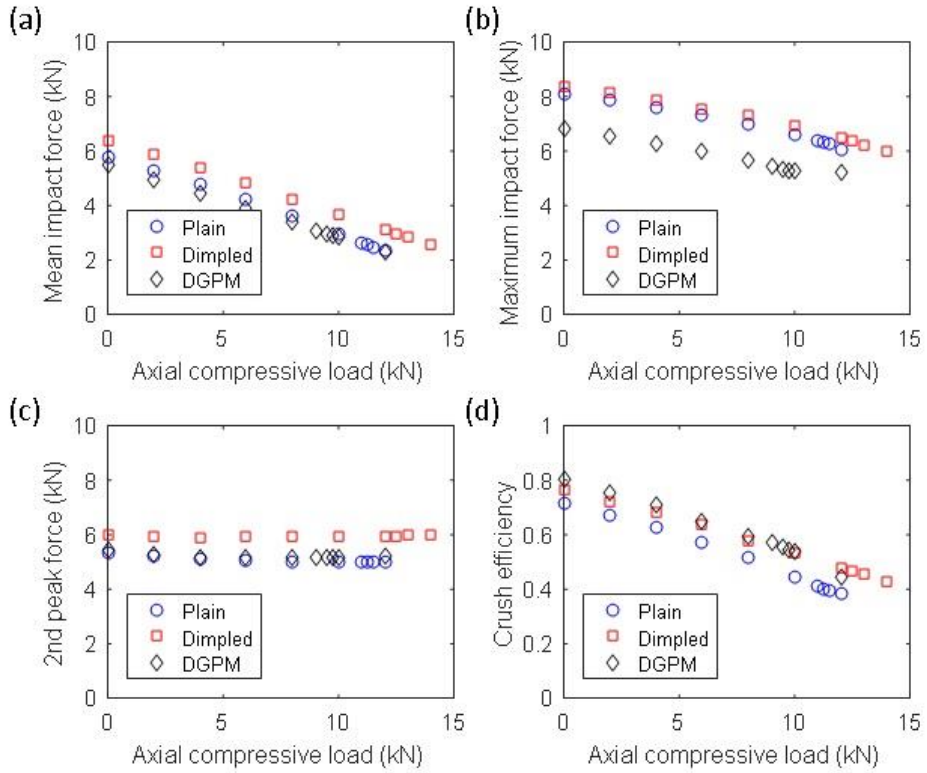

Fig. 12. (a) Mean force, (b) maximum peak force, (c) 2nd peak force and (d) crush efficiency under different axial compressive loads

Material	Axial compressive load P (kN)	Mean impact force P_{mean}(kN)	Maximum impact force P_{max} (kN)	Crush efficiency P_{mean}/P_{max}	Stability	Critical compressive load P_c (kN)	P_c/P_y
Plain	0	5.76	8.08	71.3%	Y	11.25	30.7 %
	2	5.27	7.87	67.0%	Y		
	4	4.77	7.62	62.6%	Y		
	6	4.21	7.34	57.4%	Y		
	8	3.62	7.01	51.6%	Y		
	10	2.95	6.62	44.6%	Y		
	12	2.34	6.07	38.5%	N		
Dimpled	0	6.39	8.36	76.5%	Y	12.50	30.2 %
	2	5.89	8.18	72.0%	Y		
	4	5.36	7.85	68.3%	Y		
	6	4.81	7.56	63.7%	Y		
	8	4.23	7.30	57.9%	Y		
	10	3.67	6.91	53.1%	Y		
	12	3.10	6.47	47.9%	Y		
DGPM	0	5.48	6.82	80.4%	Y	9.75	29.5 %
	2	4.96	6.57	75.5%	Y		
	4	4.45	6.26	71.1%	Y		
	6	3.91	6.01	65.1%	Y		
	8	3.37	5.67	59.5%	Y		
	10	2.82	5.25	53.7%	N		
	12	2.31	5.19	44.5%	N		

Table 1. Summary of the numerical results

3.3 Parametric study: effects of the support conditions

The plain, dimpled and DGPM structural members were analysed under two additional support conditions to further investigate the behaviour under lateral impact loads. The two additional support conditions are fully fixed at both ends, and roller supported at both ends, both without axial compressive loads. As no axial compressive loads has been applied in this section, the structural members would behave as beams. However, for the purpose of maintaining consistency, they are still referred as columns in this section. The mean forces, peak forces and crush efficiencies for three types of columns under two support conditions are presented in Fig. 13. It is found that the crush efficiencies of dimpled and DGPM columns are both 6.4% higher than the plain one when the samples are fully fixed at both ends, whereas the crush efficiencies of three columns are nearly identical when the samples are roller supported at both ends. Through comparing the mean and peak forces, it is noticed that the difference in crush efficiencies are mainly caused by peak forces. The advantage of dimpled and DGPM columns in crush efficiency is mainly due to the relatively lower peak impact forces, vice versa. When the columns are fixed supported at both ends, peak forces can be observed when the fixed ends started yielding. The propagation of yielding effect of dimpled and plain columns is shown in Fig. 14. The yielding effect near the dimpled columns fixed ends develops from the valley regions of dimples. A similar phenomenon can be observed in DGPM columns, too. Comparing to the continuous yielding effect in plain columns, the discrete yielding effect in dimpled and DGPM columns is in favour of reducing the peak impact force. By contrast, the material near both ends do not experience yielding effects under the roller-roller support condition, and the yielding effect is observed only near the impact location (i.e. mid-span) when peak forces appears. As shown in Fig. 15, the development of yielding effect in plain

and dimpled columns are similar. Therefore, the advantage of dimpled and DGPM columns in peak impact force no longer exists.

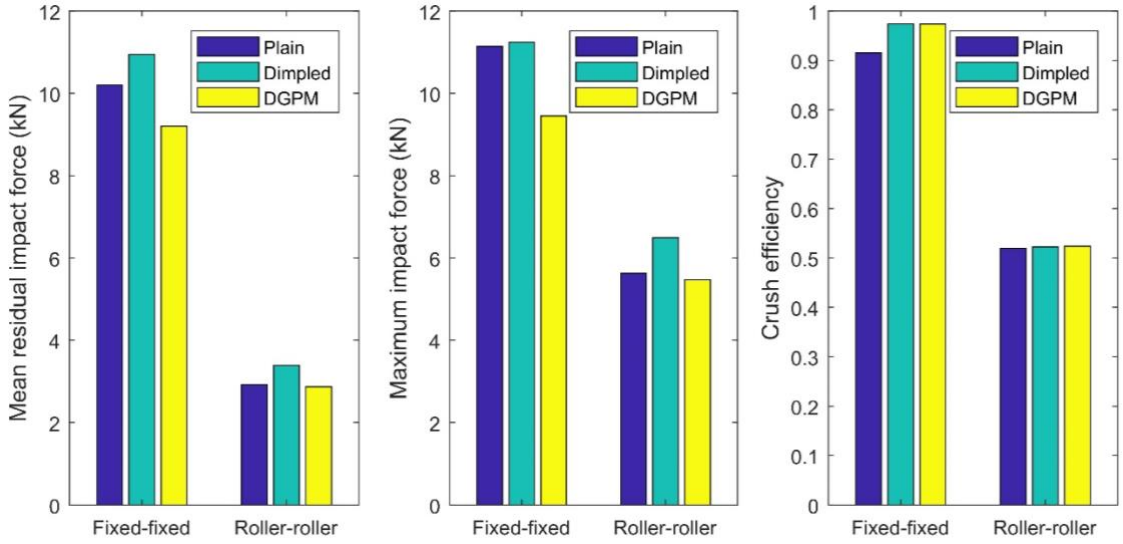

Fig. 13. (a) Mean force, (b) peak force and (c) crush efficiency under fixed-fixed and roller-roller support conditions

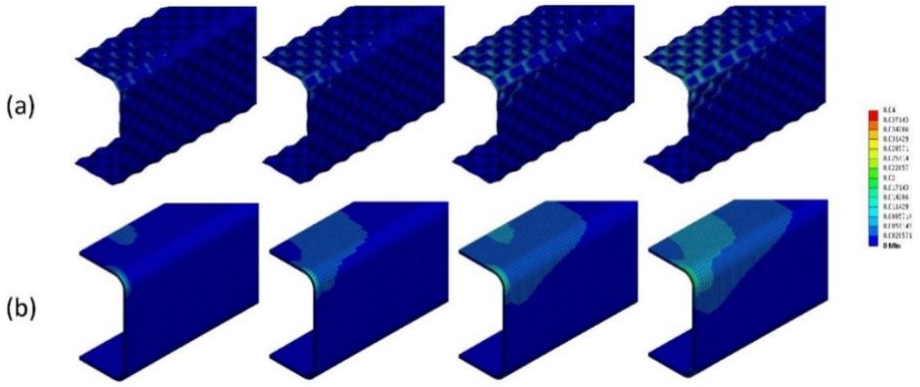

Fig. 14. Propagation of yielding effect in fixed-fixed supported (a) dimpled and (b) plain columns when the peak impact force appeared

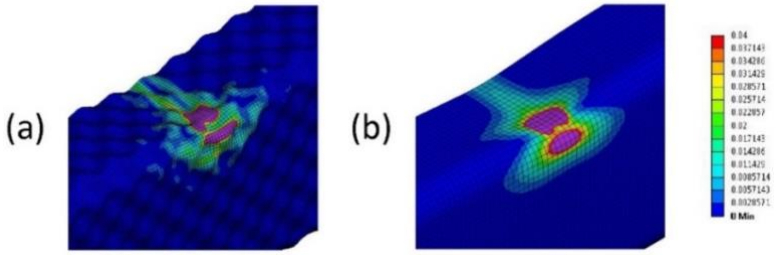

Fig. 15. Plastic strain near the impact location of roller-roller supported (a) dimpled and (b) plain columns when the peak impact force appeared

4. Conclusions

In this study, FE simulations were conducted to investigate the behaviour of dimpled columns subjected to lateral impact loads. Plain, dimpled and DGPM columns were analysed and compared. An impact mass of 4.9 kg and an impact velocity of 8 m/s were applied at columns' mid-span in all cases. The columns were fully fixed at one end and roller supported at the other end in majority cases. The core findings of this study were summarised as below:

- An initial peak impact force can be observed in plain columns when the contact started. However, the 1st peak force for dimpled and DGPM columns can be neglected. The reason is that initiation of the yielding effect is slower in dimpled and DGPM columns, due to the dimpled geometry. Additionally, the development of yielding effect near the fixed end in plain columns is faster than in dimpled and DGPM columns.
- As the axial compressive loads increasing, mean force, maximum impact force and crush efficiency gradually decrease, while change in the 2nd peak force can be neglected. The mean force and crush efficiency of dimpled columns are up to 32.5% and 24.4% greater than the equivalent plain ones, respectively. The advantage of dimpled columns in mean force and crush efficiency is generally more significant under higher axial compressive loads.
- Dimpled columns have shown better stability under combined axial compressive and lateral impact loads. Dimpled columns are capable of taking an up to 11.1% greater axial compressive load than equivalent plain ones before losing stability.
- Comparing with plain columns, the advantage of dimpled columns in crush efficiency was noted under the fixed-fixed support condition but not under the

roller-roller support condition. It was found that the dimpled geometry contributed in reducing peak impact force in the event that column ends experienced yielding effect. The dimpled geometry or similar features can be considered in structural components to increase the crush efficiency.

References

[1] M. Bambach, H. Jama, X. Zhao, R. Grzebieta. Hollow and concrete filled steel hollow sections under transverse impact loads. Eng. Struct. 2008;30: 2859-2870.

[2] I. Harik, A. Shaaban, H. Gesund, G. Valli, S. Wang. United States bridge failures, 1955-1988. J. Perform Constr. Facil. 1990;4: 272-277.

[3] K. Wardhana, F.C. Hadipriono. Analysis of recent bridge failures in the United States. J. Perform Constr. Facil. 2003;17: 144-150.

[4] H. Al-Thairy, Y.C. Wang. A numerical study of the behaviour and failure modes of axially compressed steel columns subjected to transverse impact. Int. J. Impact Eng. 2011;38: 732-744.

[5] D. Kecman. Bending collapse of rectangular and square section tubes. Int. J. Mech. Sci. 1983;25(9-10): 626-636.

[6] J.H. Liu, N. Jones. Experimental investigation of clamped beams struck transversely by a mass. Int. J. Impact. Eng. 1987;6(4): 303-335.

[7] J. Yu, N. Jones. Further experimental investigation on the failure of clamped beams under impact loads. Int. J. Solid Struct. 1991;27(9): 1113-1137.

[8] T. Wierzbicki, L. Recke, W. Abramowicz, T. Guolami, J. Huang. Stress profile in thin-walled prismatic columns subjected crush loading - II. Computers & Structures 1994;51(6): 625-641.

[9] M. Zeinoddini, G.A.R. Parke, J.E. Harding. Axially pre-loaded steel tubes subjected to lateral impacts: an experimental study. Int. J. Impact Eng. 2002;27: 669-690.

[10] M. Zeinoddini, J.E. Harding, G.A.R. Parke. Axially pre-loaded steel tubes subjected to lateral impacts (a numerical study). Int. J. Impact Eng. 2008;35: 1267-1279.

[11] S. Santosa, T. Wierzbicki. Effect of an ultralight metal filler on the bending collapse behaviour of thin-walled prismatic columns. Int. J. Mech. Sci. 1999;41(8): 995-1019.

[12] J. Fang, Y. Gao, G. Sun, Y. Zhang, Q. Li. Parametric analysis and multi objective optimization for functionally graded foam-filled thin-walled tube under lateral impact. Computational Mater. Sci. 2014;90: 265-275.

[13] R. Wang, L.H. Han, C.C. Hou. Behaviour of concrete filled steel tubular (CFST) members under lateral impact: Experiment and FEA model. J. Constr. Steel Res. 2013;80:188-201.

[14] M. Yousuf, B. Uy, Z. Tao, A. Remennikov, J.Y.R. Liew. Transverse impact resistance of hollow and concrete filled stainless steel columns. J. Const. Steel Res. 2013;82:177-189.

[15] M. Yousuf, B. Uy, Z. Tao, A. Remennikov, J.Y.R. Liew. Impact behaviour of pre-compressed hollow and concrete filled mild and stainless steel columns. J. Constr. Steel Res. 2014;96: 54-68.

[16] Y. Wang, X. Qian, J.Y.R. Liew, M.H. Zhang. Experimental behaviour of cement filed pipe-in-pipe composite structures under transverse impact. Int. J. Impact Eng. 2014;72: 1-16.

[17] J.C. Teng, J.F. Chen, S.T. Smith, L. Lam. FRP – strengthened RC structures. West Sussex, UK: John Wiley & Sons, Ltd. 2001.

[18] S. Rizkalla, T. Hassan, N. Hassan. Design recommendations for the use of FRP for reinforced and strengthening of concrete structures. Prog. Struct. Eng. Mater. 2003;5: 16-28.

[19] M.I. Alam, S. Fawzia. Numerical studies on CFRP strengthened steel under transverse impact. Composite Struct. 2015;120: 428-441.

[20] Hadley Industries plc, PO Box 92, Downing Street, Smethwick, West Midlands, B66 2PA, UK.

[21] J. Collins, M.A. Castellucci, I. Pillinger, P. Hartley. The influence of tool design on the development of localised regions of plastic deformation in sheet metal formed products to improve structural performance. In: Proceedings of the tenth international conference on metal forming; 2004. p. 68.

[22] V.B. Nguyen, C.J. Wang, D.J.Mynors, M.A. English, M.A. Castellucci. Dimpling process in cold roll metal forming by finite element modelling and experimental validation. J. Manuf. Process 2014;16:363-372.

[23] C. Liang, C.J. Wang, V.B. Nguyen, M. English, D. Mynors. Experimental and numerical study on crashworthiness of cold-formed dimpled steel columns. Thin-Walled Struct. 2017;112: 83-91.

[24] V.B. Nguyen, C.J. Wang, D.J. Mynors, M.A. Castellucci, M.A. English. Finite Element simulation on mechanical and structural properties of cold-formed dimpled steel. Thin-Walled Struct.2013;64:13-22.

[25] V.B. Nguyen, C.J. Wang, D.J. Mynors, M.A. English, M.A. Castellucci. Mechanical behaviour of cold-rolled formed dimpled steel. Steel Res. Int. 2011; Special Issue: 1072-1077.

[26] V.B. Nguyen, D.J. Mynors, C.J. Wang, M.A. Castellucci, M.A. English. Analysis and design of cold-formed dimpled steel columns using Finite Element techniques. Finite Elem. Anal. Des.2016;108:22-31.

[27] V.B. Nguyen, C.J. Wang, D.J. Mynors, M.A. English, M.A. Castellucci. Compression tests of cold-formed plain and dimpled steel columns. J. of Constr. Steel Res.2012;49:20-29.

[28] ANSYS® Academic Research, Release 17.1.

[29] British Standard, BS EN 10002-1:2001. Metallic materials - Tensile testing - Part 1: Method of test at ambient temperature; 2001.